8 October 2002

Quasiequilibrium Sequences of Binary Neutron Stars

Keisuke Taniguchi

Department of Earth and Astronomy,
Graduate School of Arts and Sciences,
University of Tokyo

§1. Introduction

A common misconception outside of the gravitational-wave research community is that the primary purpose of observatories such as LIGO is to detect directly gravitational waves. Although the first unambiguous direct detection will certainly be a celebrated event, the real excitement will come when gravitational-wave detection can be used as an observational tool for astronomy.

(S. A. Hughes, et al., astro-ph/0110349)

Detection of gravitational waves

- Dynamics of strong gravitational field
- Physics in high density regions
- Black hole formations / Neutron star formations
- Proof of general relativity in the strong gravitational field
- Cosmology
- etc.

Laser interferometers

Ground-based detectors

LIGO (USA) http://www.ligo.caltech.edu/

The data taking has just started.

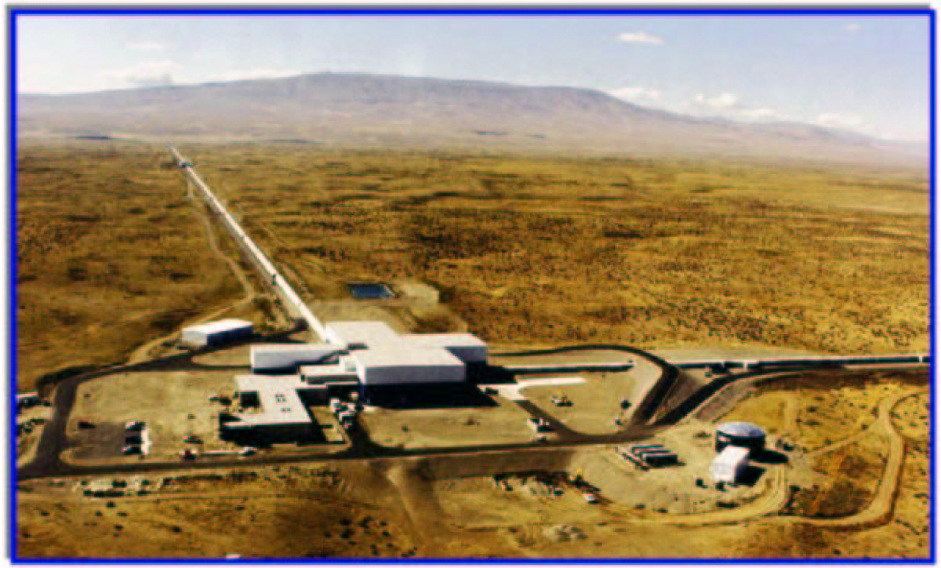

Hanford, Washington, USA
4km, 2km

Livingston, Louisiana, USA
4km

VIRGO (France & Italy) http://www.pg.infn.it/virgo/

The operation has not started yet.

Pisa, Italy
3km

GEO600 (England & Germany) http://www.geo600.uni-hannover.de/

The data taking has just started.

Hannover, Germany
600m

TAMA300 (Japan) http://tamago.mtk.nao.ac.jp/

The data taking has started since summer in 1999.

Mitaka, Tokyo, Japan

300km

Space-based detectors

LISA (ESA & NASA) http://www.lisa.uni-hannover.de/

It may launch in 2011.

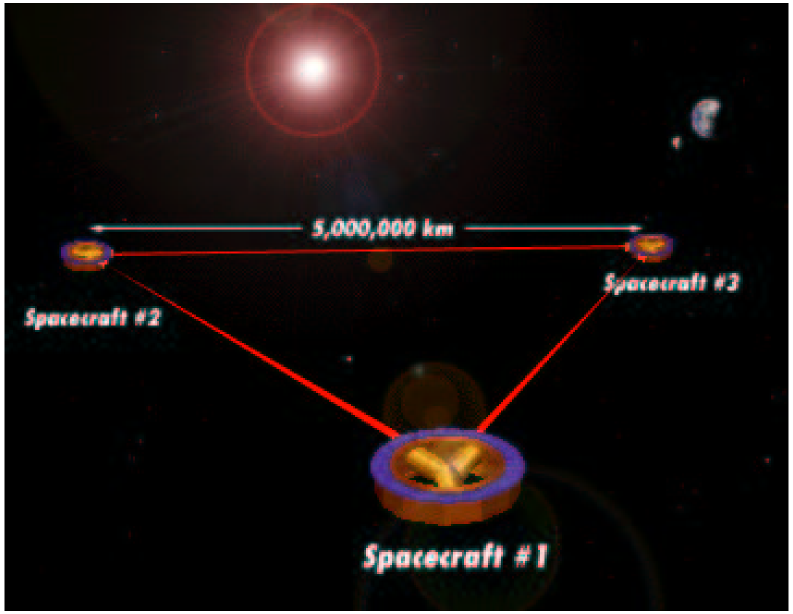

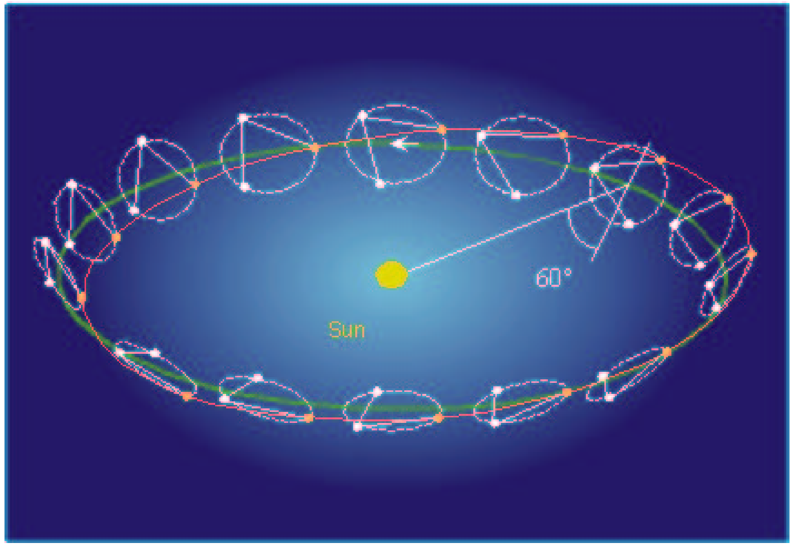

5000000km

Targets for laser interferometers

For ground-based detectors

- Coalescing compact binaries (NS-NS, NS-BH, BH-BH)
- Oscillation of neutron stars
- Rapidly rotating neutron stars
- Stellar core collapse (supernovae)
- Low-mass X-ray binaries
- etc.

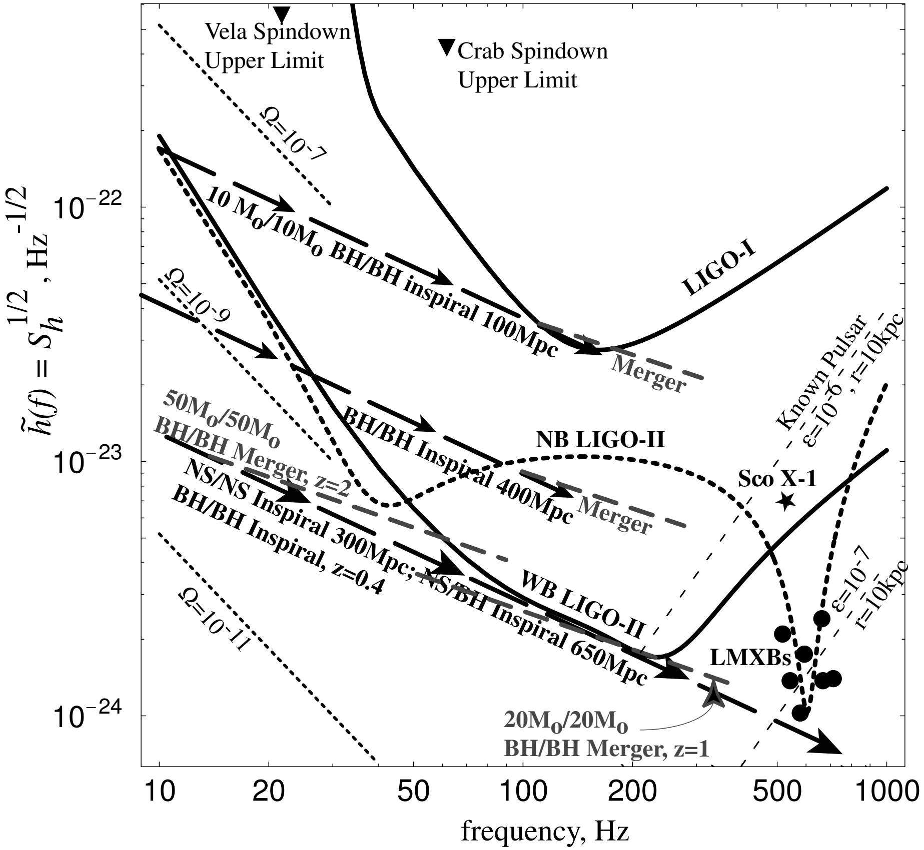

C. Cutler & K. S. Thorne, Proceeding of GR16 (2002), gr-qc/0204090

For space-based detector

- Short-period galactic binaries (WD-WD, WD-LMHS, Low-mass X-ray binaries)
- Inspiral and merger of supermassive black hole binaries
- Inspiral and capture of compact objects by supermassive black holes
- Collapse of supermassive stars
- etc.

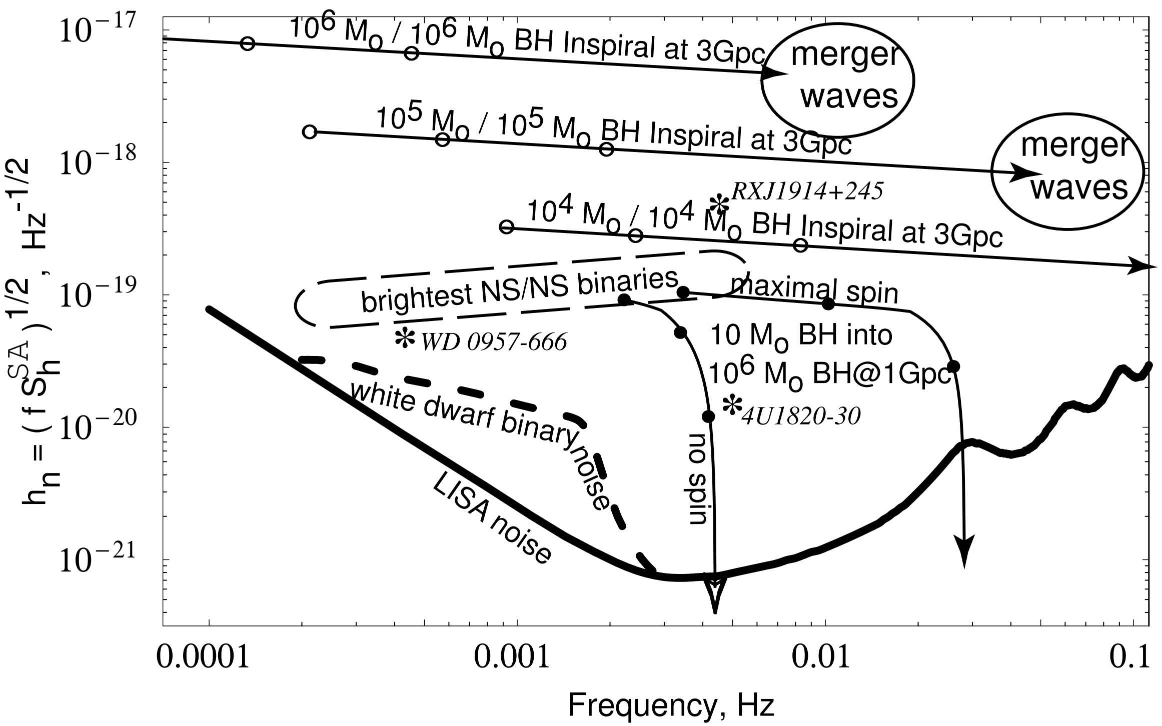

C. Cutler & K. S. Thorne, Proceeding of GR16 (2002), gr-qc/0204090

§2. Evolution of binary neutron stars

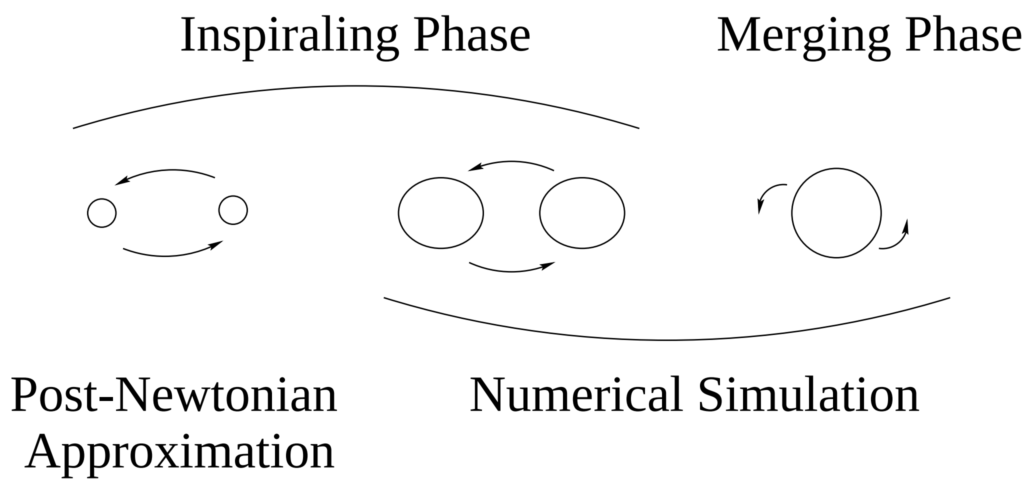

Inspiraling phase

Mass and Spin of each NS, etc.

Blanchet, Damour, Schäfer, $\cdots$

Intermediate phase

Initial data for merging phase, Eq. of state of each NS, etc.

Bonazzola, Gourgoulhon, Marck & KT
Uryū, Eriguchi & Usui
Wilson, Mathews, & Marronetti, $\cdots$

Merging phase

Eq. of state of each NS, BH formation, etc.

Shibata
Oohara & Nakamura
Washington University group, $\cdots$

§3. Formulation

§§3.1 Basic assumptions

Quasiequilibrium

$$\frac{t_{\rm GW}}{P_{\rm orb}} \simeq 1.1 \left(\frac{c^2 d}{6GM_{\rm tot}} \right)^{5/2} \left(\frac{M_{\rm tot}}{4\mu} \right)$$

We assume that there exists a Killing vector:

$$\boldsymbol{l} = \frac{\partial}{\partial t} + \Omega \frac{\partial}{\partial \varphi}$$

Perfect fluid

The matter stress-energy tensor:

$$T_{\mu\nu} = (e+p)u_\mu u_\nu + p g_{\mu\nu}$$

Synchronized and irrotational flow

The realistic rotation state will be irrotational one.

C. S. Kochaneck, ApJ. **398**, 234 (1992).
L. Bildsten & C. Cutler, ApJ. **400**, 175 (1992).

Polytropic equation of state

$$p = \kappa \rho^\gamma$$

Conformally flat spatial metric

(Isenberg-Wilson-Mathews approximation)

A simplifying assumption for the metric:

$$ds^2 = -(N^2 - B_i B^i) dt^2 - 2B_i dt dx^i + A^2 f_{ij} dx^i dx^j$$

§§3.2 Basic equations

Fluid equations

First integral of fluid motion:

$$H + \nu - \ln\Gamma_0 + \ln\Gamma = \text{constant}$$

Differential eq. for the velocity potential of irrotational flow:

$$\zeta H \underline{\Delta}\Psi_0 + \left[(1-\zeta H)\bar\nabla^i H + \zeta H \bar\nabla^i\beta\right]\bar\nabla_i\Psi_0$$
$$= (W^i - W_0^i)\bar\nabla_i H + \zeta H\left[W_0^i\bar\nabla_i(H-\beta) + \frac{W^i}{\Gamma_n}\bar\nabla_i\Gamma_n\right]$$

Gravitational field equations

The trace of the spatial part of the Einstein eq. combined with the Hamiltonian constraint eq.:

$$\underline{\Delta}\nu = 4\pi A^2(E+S) + A^2 K_{ij}K^{ij} - \bar\nabla_i\nu\bar\nabla^i\beta$$
$$\underline{\Delta}\beta = 4\pi A^2 S + \frac{3}{4}A^2 K_{ij}K^{ij} - \frac{1}{2}(\bar\nabla_i\nu\bar\nabla^i\nu + \bar\nabla_i\beta\bar\nabla^i\beta)$$

Momentum constraint equation:

$$\underline{\Delta}N^i + \frac{1}{3}\bar\nabla^i(\bar\nabla_j N^j) = -16\pi N A^2(E+p)U^i + 2NA^2K^{ij}\bar\nabla_j(3\beta - 4\nu)$$

$H := \ln h$
h : fluid specific enthalpy
$\nu := \ln N$
$\beta := \ln(AN)$
Γ_0 : Lorentz factor between the co-orbiting observer and the Eulerian one
Γ : Lorentz factor between the fluid and the co-orbiting observer
Γ_n : Lorentz factor between the fluid and the Eulerian observer
Irrot. fluid 4-velocity: $\mathbf{u} = \frac{\nabla\Psi}{h}$
Scalar potential: $\Psi = \Psi_0 + f_{ij}W_0^i x^j$
$E := \Gamma_n^2(e+p) - p$
$S := 3p + (E+p)U^iU_i$
$N^i = B^i + (\mathbf{\Omega}\times\mathbf{r})^i$
U^i : fluid 3-velocity w.r.t. the Eulerian observer

$$\zeta = \frac{d\ln H}{d\ln n}$$

§4 Numerical method

Spectral methods lose much of their accuracy when non-smooth functions are treated because of the so-called Gibbs phenomenon.

> For a $\mathcal{C}^\infty$ function, the numerical error decreases as $\exp(-N)$, where N is the number of coefficients involved in the spectral expansion. On the other hand, the coefficients of a function which is of class $\mathcal{C}^p$ but not $\mathcal{C}^{p+1}$ decrease as $1/N^p$ only.

$\Uparrow$

Multi-domain spectral method circumvents it.

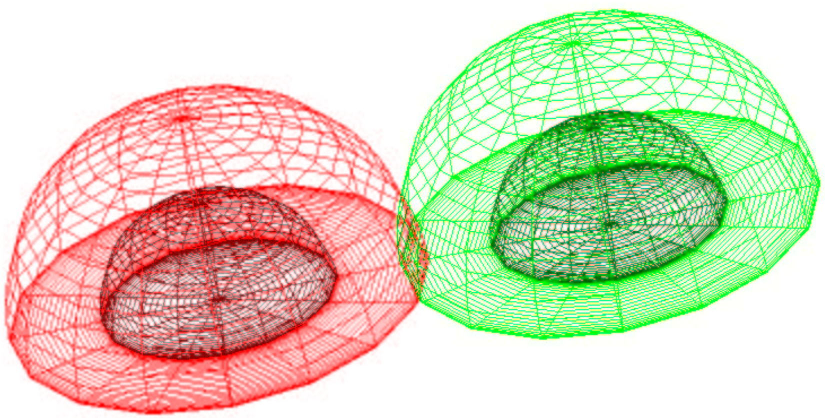

§§4.1 Multi-domain spectral method

S. Bonazzola, E.Gourgoulhon & J.-A. Marck, PRD **58**, 104020 (1998); J. Comput. Appl. Math. **109**, 433 (1999).

P. Grandclément, S. Bonazzola, E. Gourgoulhon & J.-A. Marck, J. Comput .Phys. **170**, 231 (2001).

Physical domains and their mapping:

Nucleus

$$[0,1]\times[0,\pi]\times[0,2\pi[\quad \longrightarrow \quad \mathcal{D}_0$$
$$(\xi,\theta',\varphi') \to (r,\theta,\varphi)$$
$$r = R_0(\xi,\theta',\varphi'), \quad \theta=\theta', \quad \varphi=\varphi'$$

Intermediate domains (shell)

$$[-1,1]\times[0,\pi]\times[0,2\pi[\quad \longrightarrow \quad \mathcal{D}_l$$
$$(\xi,\theta',\varphi') \to (r,\theta,\varphi)$$
$$r = R_l(\xi,\theta',\varphi'), \quad \theta=\theta', \quad \varphi=\varphi'$$

Compactified infinite domain

$$[-1,1]\times[0,\pi]\times[0,2\pi[\quad \longrightarrow \quad \mathcal{D}_{\rm ext}$$
$$(\xi,\theta',\varphi') \to (r,\theta,\varphi)$$
$$u := 1/r = U(\xi,\theta',\varphi'), \quad \theta=\theta', \quad \varphi=\varphi'$$

Spectral expansion

$$f(\xi,\theta,\varphi) = \sum_{k=0}^{N_\varphi-1}\sum_{j=0}^{N_\theta-1}\sum_{i=0}^{N_r-1} \hat{f}_{kji} X_{kji}(\xi)\Theta_{kj}(\theta)\Phi_k(\varphi)$$

N_r, N_θ, N_φ : numbers of degrees of freedom in r, θ and φ

φ direction

$$\Phi_k(\varphi) = e^{ik\varphi} \qquad (-N_\varphi/2 \le k \le N_\varphi/2)$$

Associated collocation points: $\varphi_k = \dfrac{2\pi k}{N_\varphi} \qquad (0 \le k \le N_\varphi - 1)$

θ direction

$$\Theta_{kj}(\theta) = \cos(j\theta) \qquad (0 \le j \le N_\theta - 1) \qquad \text{for } k : \text{even}$$

$$\Theta_{kj}(\theta) = \sin(j\theta) \qquad (1 \le j \le N_\theta - 2) \qquad \text{for } k : \text{odd}$$

Associated collocation points: $\theta_j = \dfrac{\pi j}{N_\theta - 1} \qquad (0 \le j \le N_\theta - 1)$

ξ direction

Nucleus

$$X_{kji}(\xi) = T_{2i}(\xi) \qquad (0 \le i \le N_r - 1) \qquad \text{for } j : \text{even}$$

$$X_{kji}(\xi) = T_{2i+1}(\xi) \qquad (0 \le i \le N_r - 2) \qquad \text{for } j : \text{odd}$$

Associated collocation points: $\xi_i = \sin\left(\dfrac{\pi}{2}\dfrac{i}{N_r - 1}\right) \qquad (0 \le i \le N_r - 1)$

Intermediate and external domains

$$X_{kji}(\xi) = T_i(\xi) \qquad (0 \le i \le N_r - 1)$$

Associated collocation points: $\xi_i = -\cos\left(\pi\dfrac{i}{N_r - 1}\right) \qquad (0 \le i \le N_r - 1)$

T_n : nth degree Chebyshev polynomial

§§4.2 Improvement on the cases of stiff EOS

If a star has a stiff EOS ($\gamma > 2$), the density decreases so rapidly that $\partial n/\partial r$ diverges at the surface.

$\Longrightarrow$ Gibbs phenomenon

$\Uparrow$

Regularization circumvents it.

Virial error for a spherical static star in Newtonian gravity

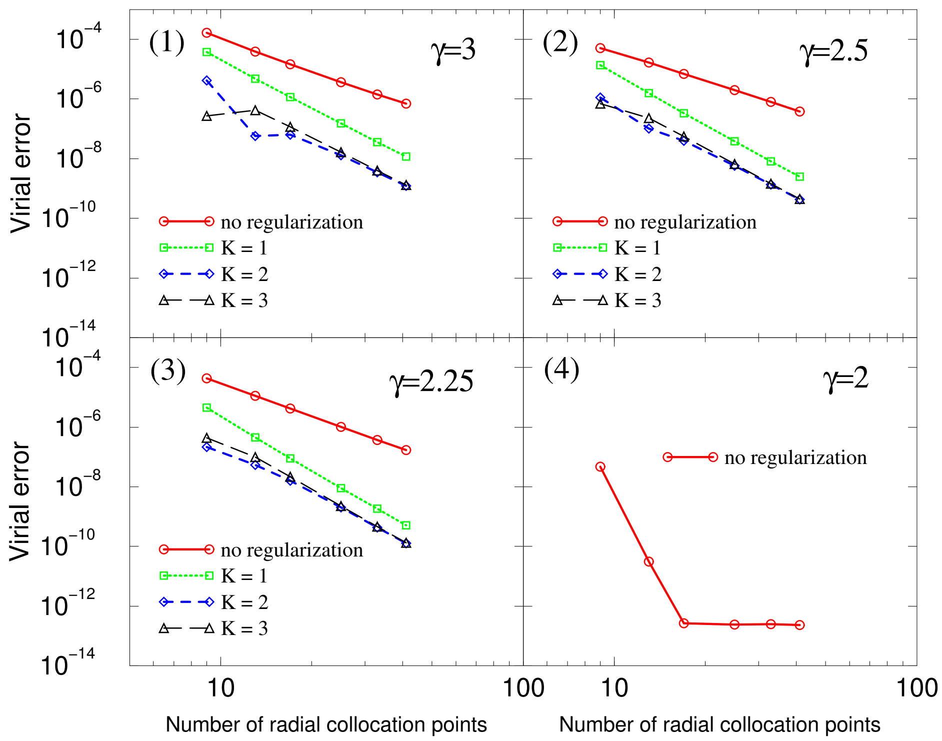

$$\text{Virial error} = \frac{|W + 3P|}{|W|}$$

W : gravitational potential energy

P : volume integral of the fluid pressure

§§4.3 Iterative procedure

(1) We prepare two numerical solutions for spherically symmetric, static, isolated neutron stars, and set the X coordinates of the two stellar centers:

$$X_{<1>} = -\frac{M_{<2>}}{M_{<1>} + M_{<2>}} d$$

and

$$X_{<2>} = \frac{M_{<1>}}{M_{<1>} + M_{<2>}} d$$

(2) We demand that the enthalpy H be maximal at the center of each star:

$$\left.\frac{\partial}{\partial X} H\right|_{(X_{<a>},0,0)} = 0, \qquad a = 1, 2$$

$\Longrightarrow \quad \Omega \quad$ and $\quad X_{\rm rot}$

(3) The X-axis is translated in order for the rotation axis to coincide with the origin of the coordinate system:

$$X_{<a>,\rm new} = X_{<a>,\rm old} - X_{\rm rot}, \qquad a = 1, 2$$

$$X_{\rm rot,new} = 0$$

(4) For irrotational configurations, the velocity potential Ψ is obtained.

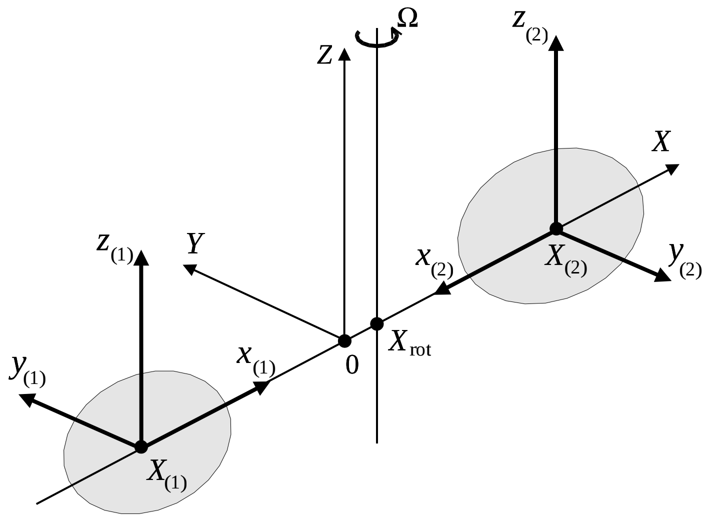

(5) The new enthalpy field is calculated: $\Longrightarrow$ We search for the location of $H = 0$ (stellar surface), and change the position of the inner domain boundary.

(6) The new baryon density and so on are obtained via the EOS.

(7) The gravitational field equations are solved.

(8) The relative difference between the enthalpy fields of two successive steps is checked:

$$\delta H := \frac{\sum_i |H^J(x_i) - H^{J-1}(x_i)|}{\sum_i |H^{J-1}(x_i)|}$$

§5. Analytical approach and tests

In the irrotational case:

In the relativistic case

Numerical solutions :

- S. Bonazzola, E. Gourgoulhon, & J.-A. Marck, PRL**82**, 892 (1999).
- E. Gourgoulhon, P. Grandclément, KT, J.-A. Marck, & S. Bonazzola, PRD**63**, 064029 (2001).
- KT & E. Gourgoulhon, accepted to PRD, gr-qc/0207098.
- K. Uryū & Y. Eriguchi, PRD**61**, 124023 (2000).
- K. Uryū, M. Shibata, & Y. Eriguchi, PRD**62**, 104015 (2000).

$\Uparrow$ Check the validity of the code

(Semi-)Analytic solutions :

Up to now, there are no solutions !

In the Newtonian case

Numerical solutions :

- K. Uryū & Y. Eriguchi, ApJS. **118**, 563 (1998).
- KT, E. Gourgoulhon, & S. Bonazzola, PRD**64**, 064012 (2001).
- KT & E. Gourgoulhon, PRD**65**, 044027 (2002).

$\Uparrow$ Check the validity of the code

Semi-analytic solutions :

- D. Lai, F. A. Rasio & S. L. Shapiro, ApJ. **420**, 811 (1994).
- KT & T. Nakamura, PRL**84**, 581 (2000); PRD**62**, 044040 (2000).

§§5.1 Newtonian analytic solution

In the irrotational case:

KT & T. Nakamura, PRL**84**, 581 (2000); PRD**62**, 044040 (2000)

Background: two spherical stars

Expansion parameter: $\epsilon := \dfrac{R_0}{d}$, d: orbital separation, R_0: radius of a star for $d \to \infty$

The physical quantities are calculated upto $O[(R_0/d)^6]$:

Equal mass: $M_1 = M_2 = M$, Polytropic index: $\gamma = 2$

Total energy

$$E = \frac{GM^2}{R_0}\left[-1-\frac{1}{2}\left(\frac{R_0}{d}\right)+2\left(\frac{15}{\pi^2}-1\right)\left(\frac{R_0}{d}\right)^6+O\left(\frac{R_0}{d}\right)^8+\cdots\right]$$

Total angular momentum

$$J = \frac{1}{2}Md^2\Omega\left[1+O\left(\frac{R_0}{d}\right)^8+\cdots\right]$$

Orbital angular velocity

$$\Omega^2 = \frac{2GM}{d^3}\left[1+6\left(\frac{15}{\pi^2}-1\right)\left(\frac{R_0}{d}\right)^5+O\left(\frac{R_0}{d}\right)^7+\cdots\right]$$

Relative change in central density

$$\delta\rho_c = \frac{\rho_c-\rho_{c0}}{\rho_c} = -\frac{45}{2\pi^2}\left(\frac{R_0}{d}\right)^6+O\left(\frac{R_0}{d}\right)^8+\cdots$$

§§5.2 Comparison with analytic solution

Global quantities

Relative difference from analytic solution

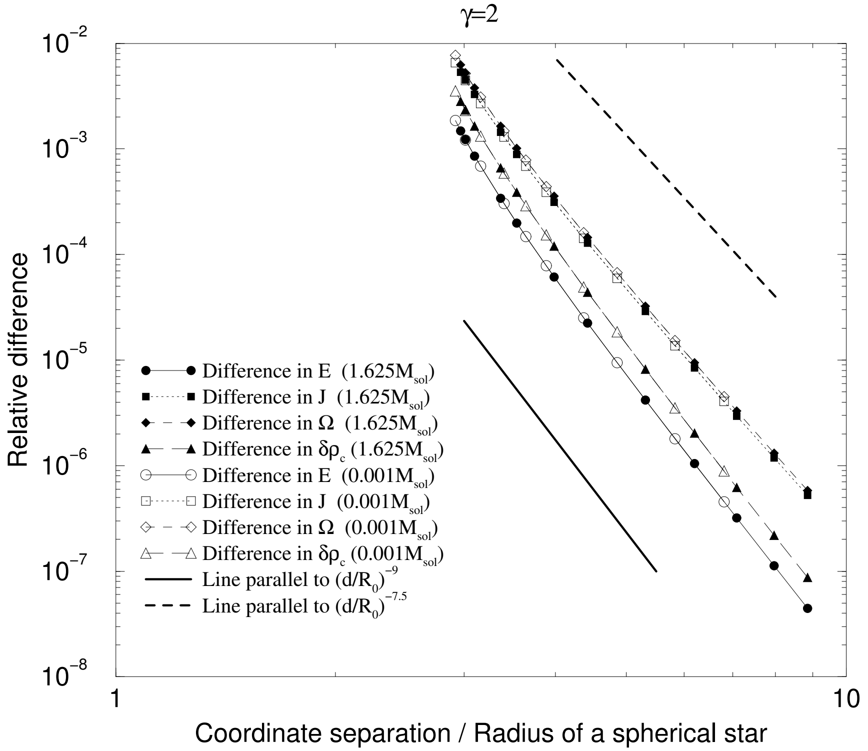

Relative difference from analytic solution

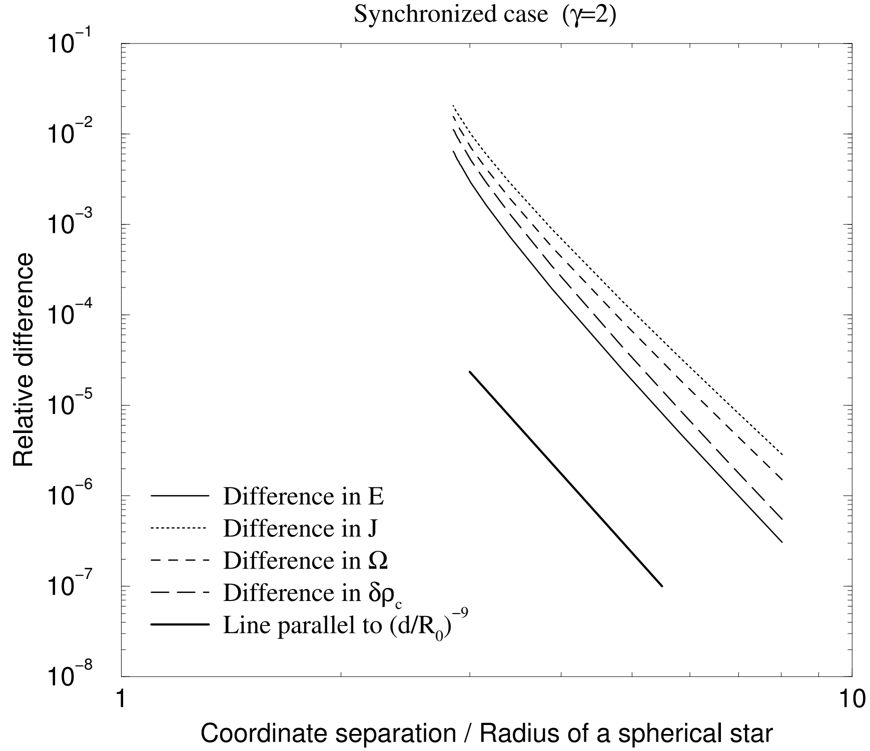

Difference in E

$$\frac{E_{\rm num} - E_{\rm ana}}{GM^2/R_0}$$

Difference in J

$$\frac{J_{\rm num} - J_{\rm ana}}{Md^2\Omega_{\rm Kep}/2}$$

Difference in Ω

$$\frac{\Omega_{\rm num} - \Omega_{\rm ana}}{\Omega_{\rm Kep}}$$

Difference in $\delta\rho_c$

$$|\delta\rho_{c:\rm num} - \delta\rho_{c:\rm ana}|$$

where $\Omega_{\rm Kep} = \left(\frac{2GM}{d^3}\right)^{1/2}$

Internal velocity field

The velocity field in the co-orbiting frame:

$$u^x = \Omega\left[\ \ y + O(\epsilon^3) + O(\epsilon^4) + O(\epsilon^5) + \cdots\right]$$

$$u^y = \Omega\left[-x + O(\epsilon^3) + O(\epsilon^4) + O(\epsilon^5) + \cdots\right]$$

$$u^z = \Omega\left[\qquad O(\epsilon^3) + O(\epsilon^4) + O(\epsilon^5) + \cdots\right]$$

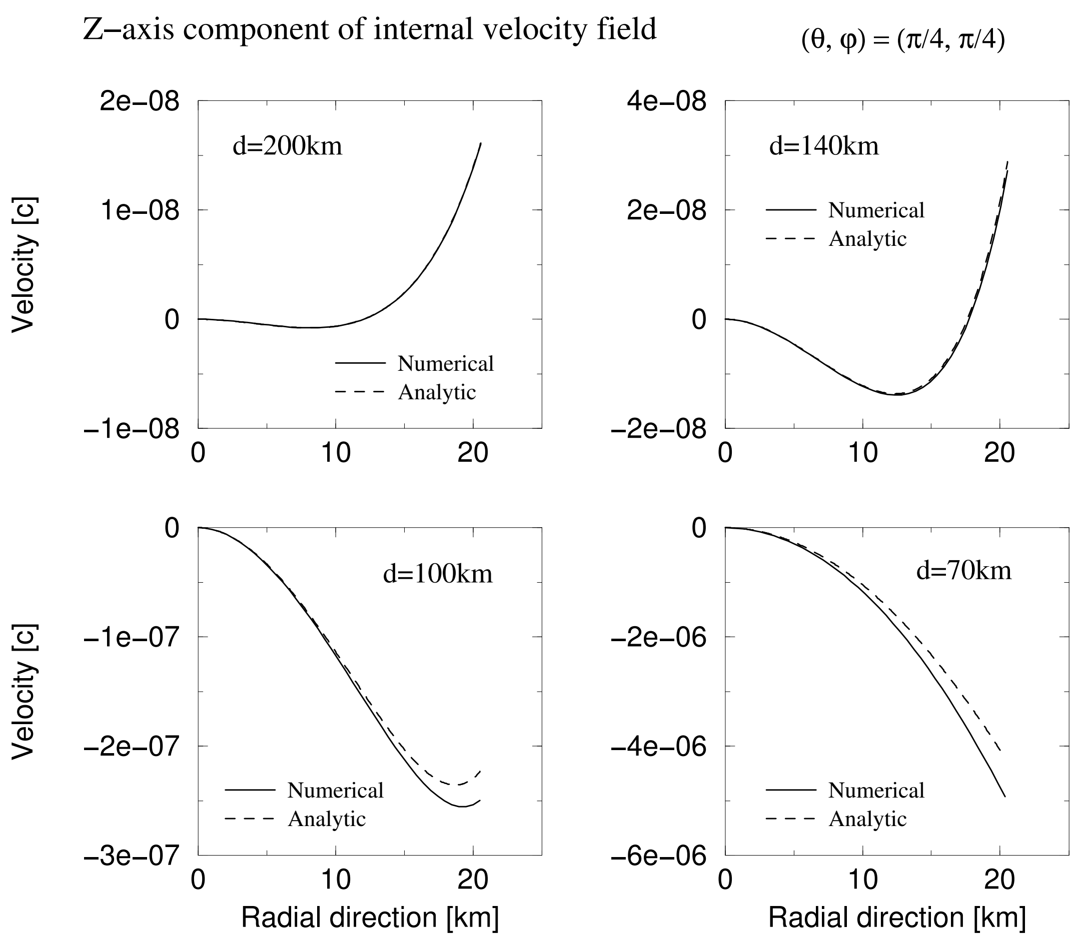

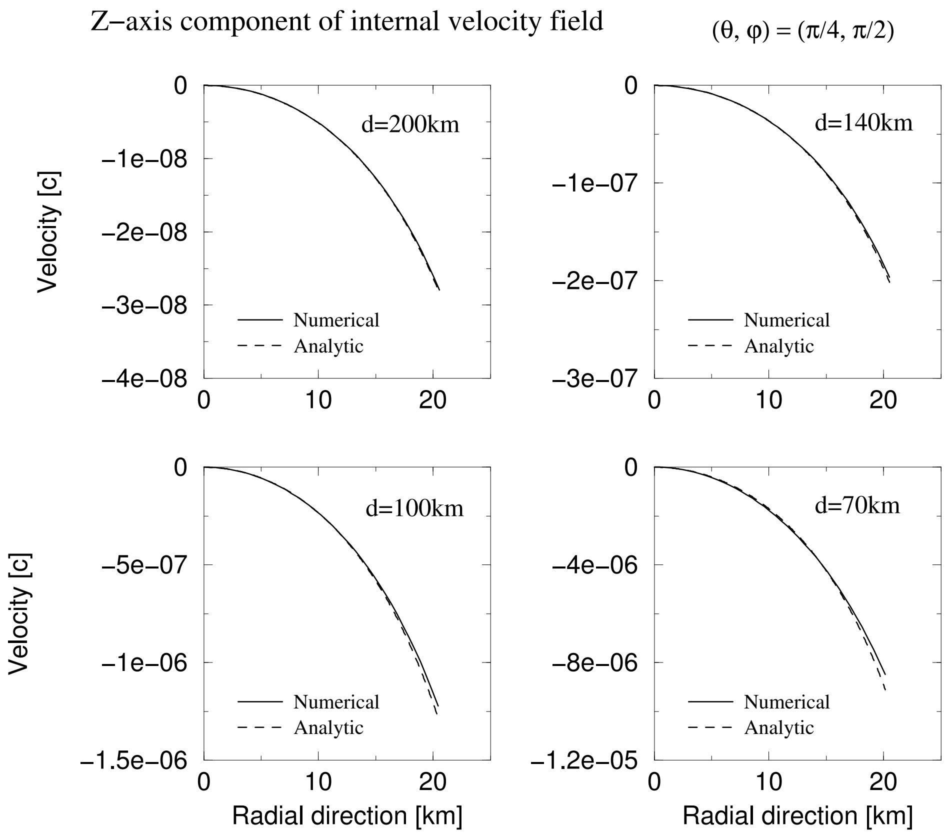

Z−axis component of internal velocity field
(θ, φ) = (π/4, π/2)
d=200km
d=140km
d=100km
d=70km
Numerical
Analytic
Velocity [c]
Radial direction [km]

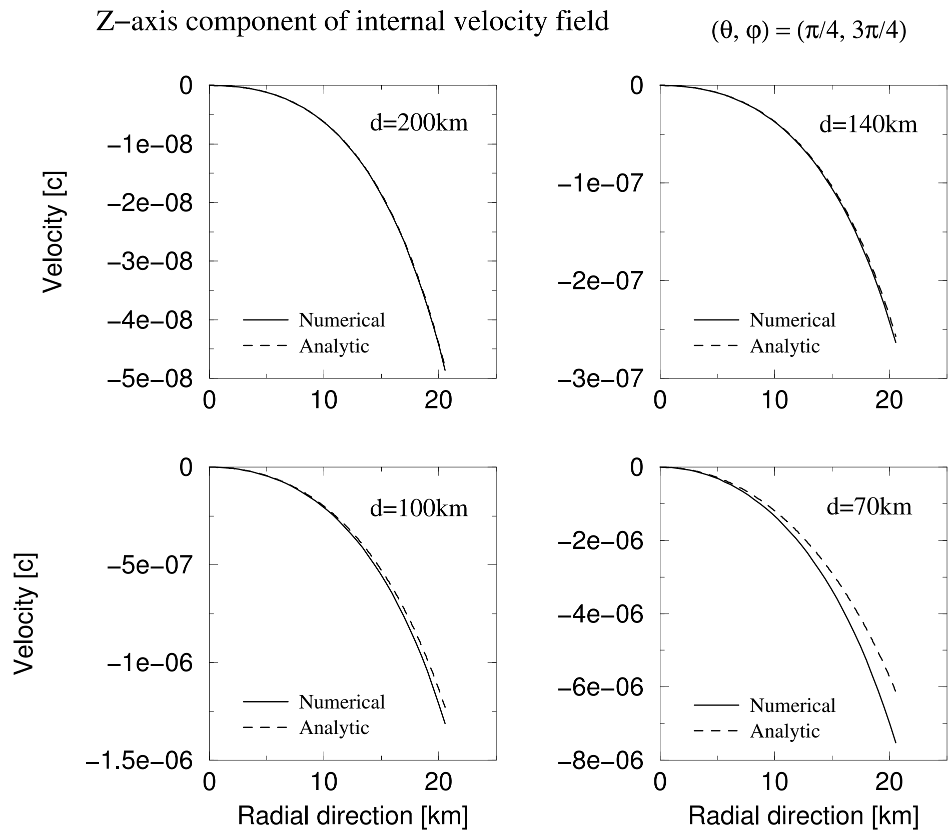

Z−axis component of internal velocity field
(θ, φ) = (π/4, 3π/4)
d=200km
d=140km
d=100km
d=70km
Numerical
Analytic
Velocity [c]
Radial direction [km]

§§5.3 Relative error in the virial theorem

Newtonian identical mass case

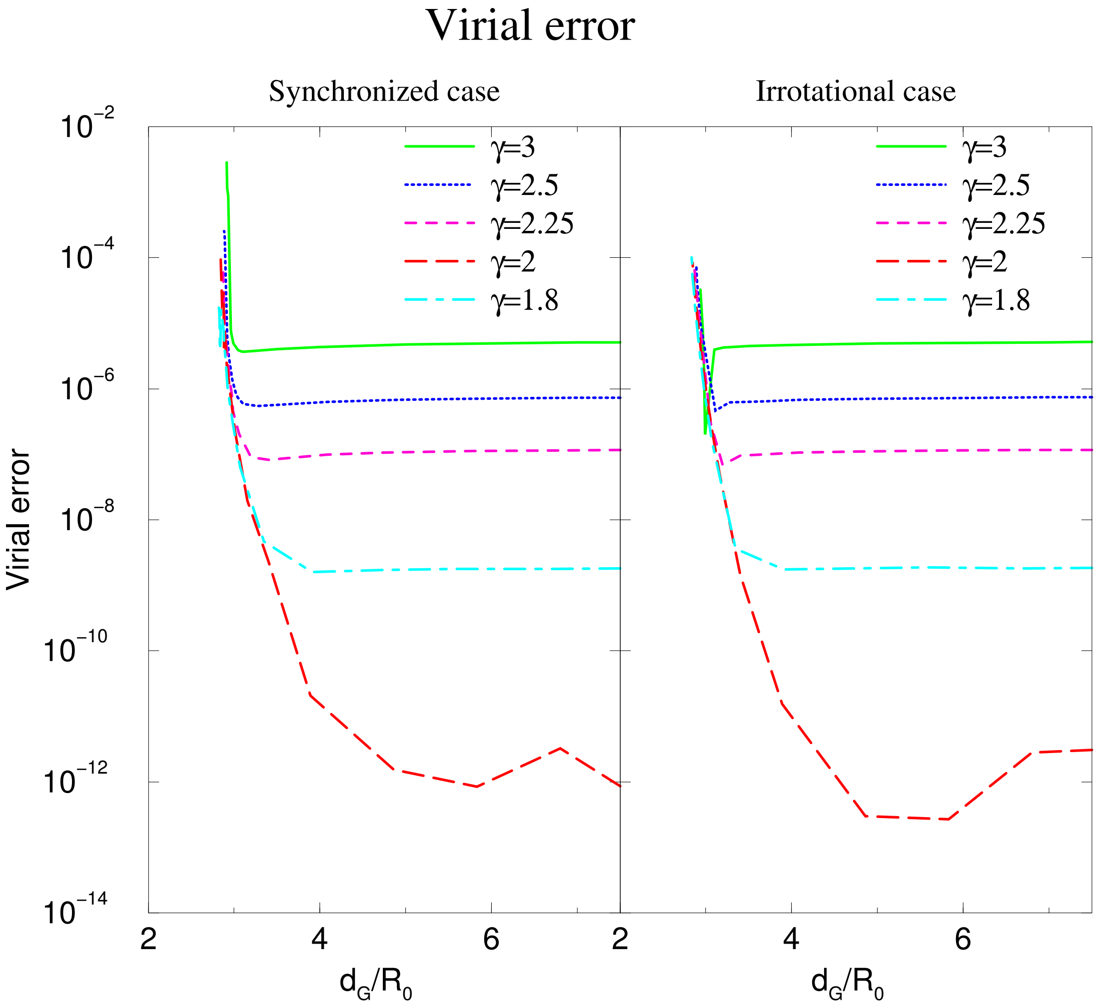

$$\text{Virial error} = \frac{|2T + W + 3P|}{|W|}$$

T : kinetic energy

W : gravitational potential energy

P : volume integral of the fluid pres-
sure

Relativistic identical mass case

Relative error in the virial theorem

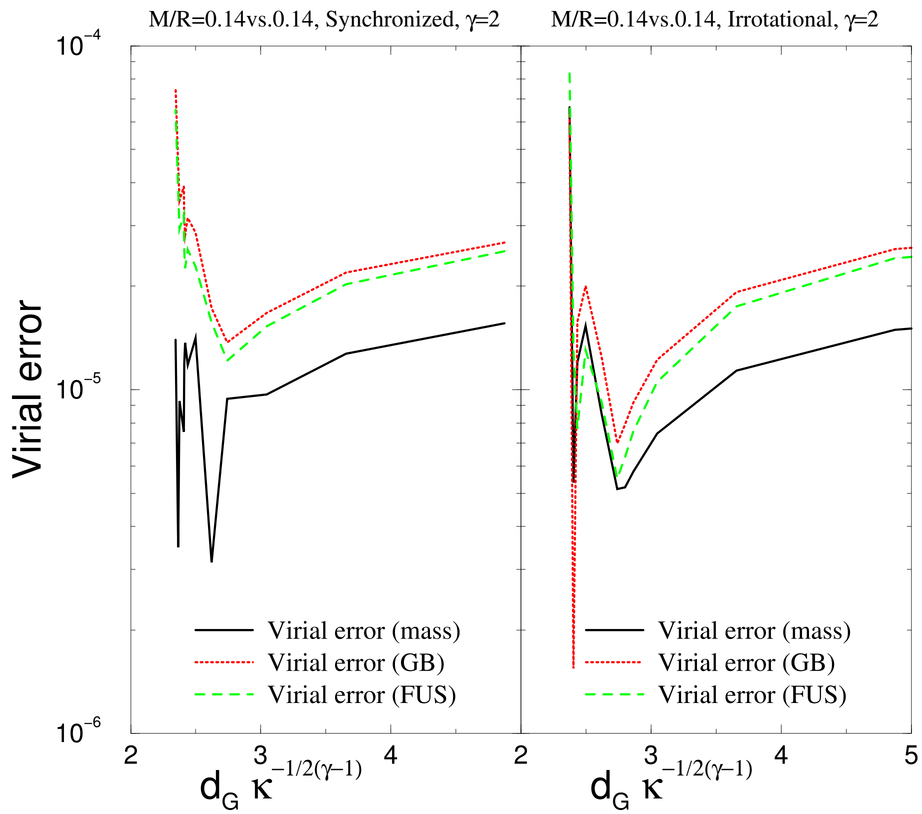

Virial error

$$\left|\frac{M_{\rm ADM}-M_{\rm Komar}}{M_{\rm ADM}}\right|$$

$$\left|\frac{VE(FUS)}{M_{\rm ADM}}\right|$$

$$\left|\frac{VE(GB)}{M_{\rm ADM}}\right|$$

ADM mass : $M_{\rm ADM} = -\dfrac{1}{2\pi}\displaystyle\oint_\infty \bar\nabla^i A^{1/2} dS_i$

Komar mass : $M_{\rm Komar} = \dfrac{1}{4\pi}\displaystyle\oint_\infty \bar\nabla^i N dS_i$

$$M_{\rm ADM} - M_{\rm Komar} = 0$$

$$VE(FUS) = \int \left[2NA^3S + \frac{3}{8\pi}NA^3K_i^jK_j^i + \frac{1}{4\pi}NA(\bar\nabla_i\beta\bar\nabla^i\beta - \bar\nabla_i\nu\bar\nabla^i\nu)\right] = 0$$

J. L. Friedman, K. Uryū, and M. Shibata, PRD**65**, 064035 (2002).

$$VE(GB) = \int \left[2A^3S + \frac{3}{8\pi}A^3K_i^jK_j^i + \frac{1}{4\pi}A(\bar\nabla_i\beta\bar\nabla^i\beta - \bar\nabla_i\nu\bar\nabla^i\nu - 2\bar\nabla_i\beta\bar\nabla^i\nu)\right] = 0$$

E. Gourgoulhon and S. Bonazzola, CQG.**11**, 443 (1994).

§6. Numerical results

Parameters

- Adiabatic index : $\gamma = 2$
- Rotation state of the binary system : synchronized and irrotational
- Compactness of the star :

$$
\begin{aligned}
M/R &= 0.12 \text{ vs. } 0.12,\ 0.12 \text{ vs. } 0.13,\ 0.12 \text{ vs. } 0.14 \\
M/R &= 0.14 \text{ vs. } 0.14,\ 0.14 \text{ vs. } 0.15,\ 0.14 \text{ vs. } 0.16 \\
M/R &= 0.16 \text{ vs. } 0.16,\ 0.16 \text{ vs. } 0.17,\ 0.16 \text{ vs. } 0.18 \\
M/R &= 0.18 \text{ vs. } 0.18
\end{aligned}
$$

Polytropic unites

$$R_{\rm poly} := \kappa^{1/2(\gamma-1)}$$

$\bar{d} := d\kappa^{-1/2(\gamma-1)}$	Coordinate separation
$\bar{\Omega} := \Omega\kappa^{1/2(\gamma-1)}$	Orbital angular velocity
$\bar{M} := M_{\rm ADM}\kappa^{-1/2(\gamma-1)}$	ADM mass
$\bar{J} := J\kappa^{-1/(\gamma-1)}$	Angular momentum

§§6.1 Equilibrium configurations

Synchronized case

$M/R = 0.14$ vs. 0.14

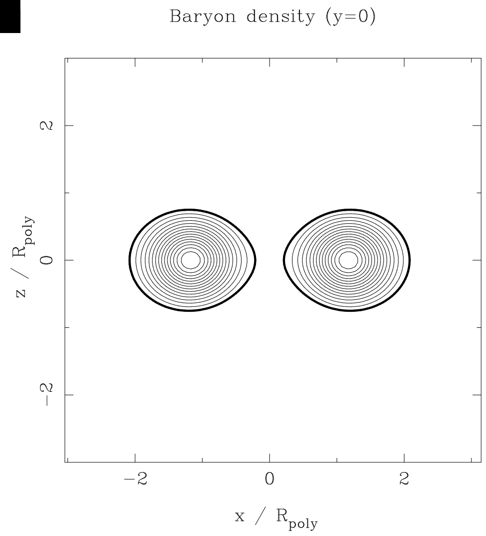

0.14 vs. 0.15

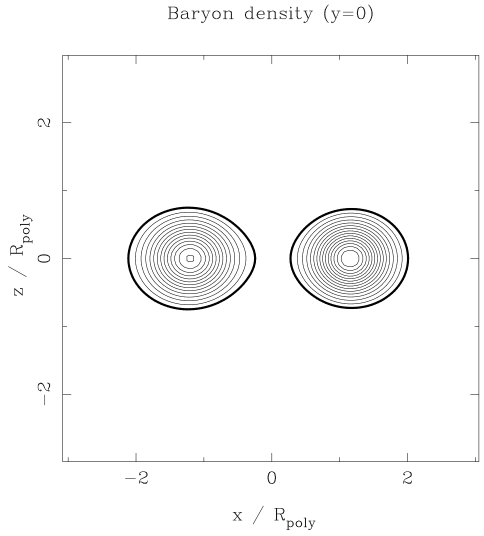

0.14 vs. 0.16

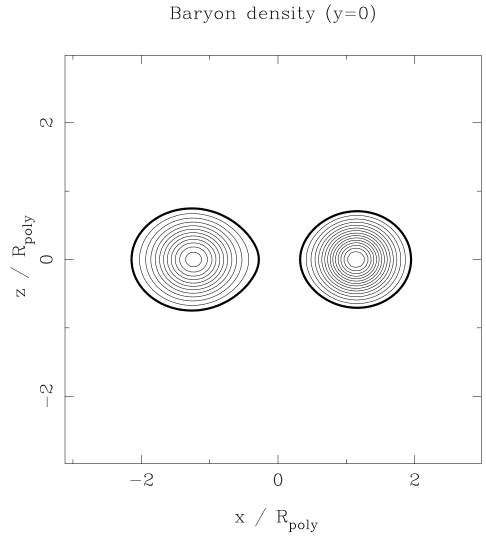

Irrotational case

$M/R = 0.14$ vs. 0.14

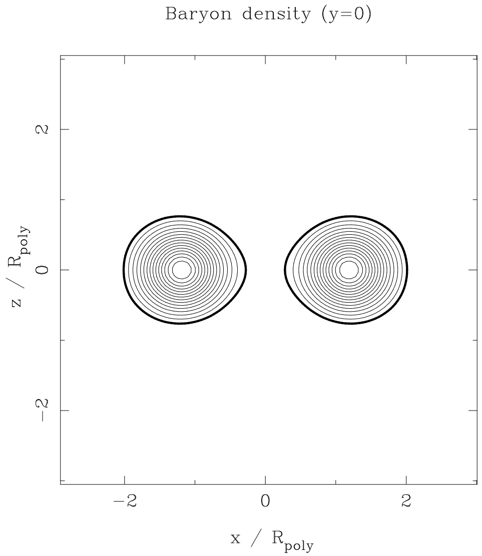

0.14 vs. 0.15

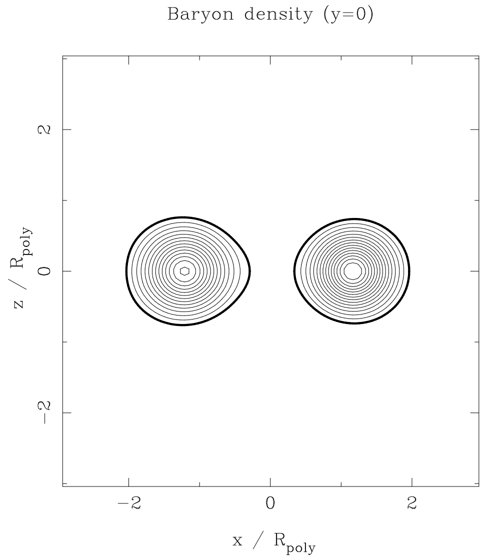

0.14 vs. 0.16

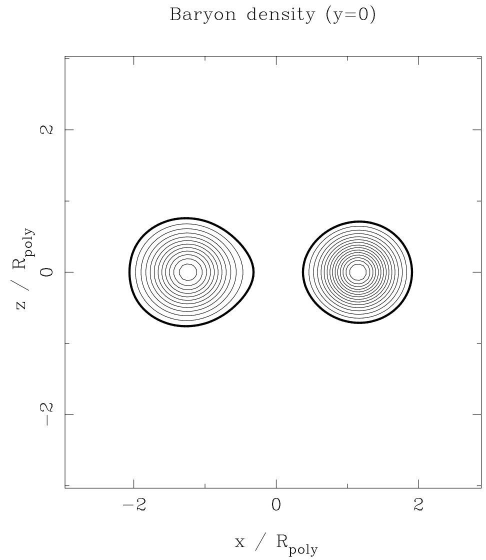

§§6.2 ADM mass

Synchronized case

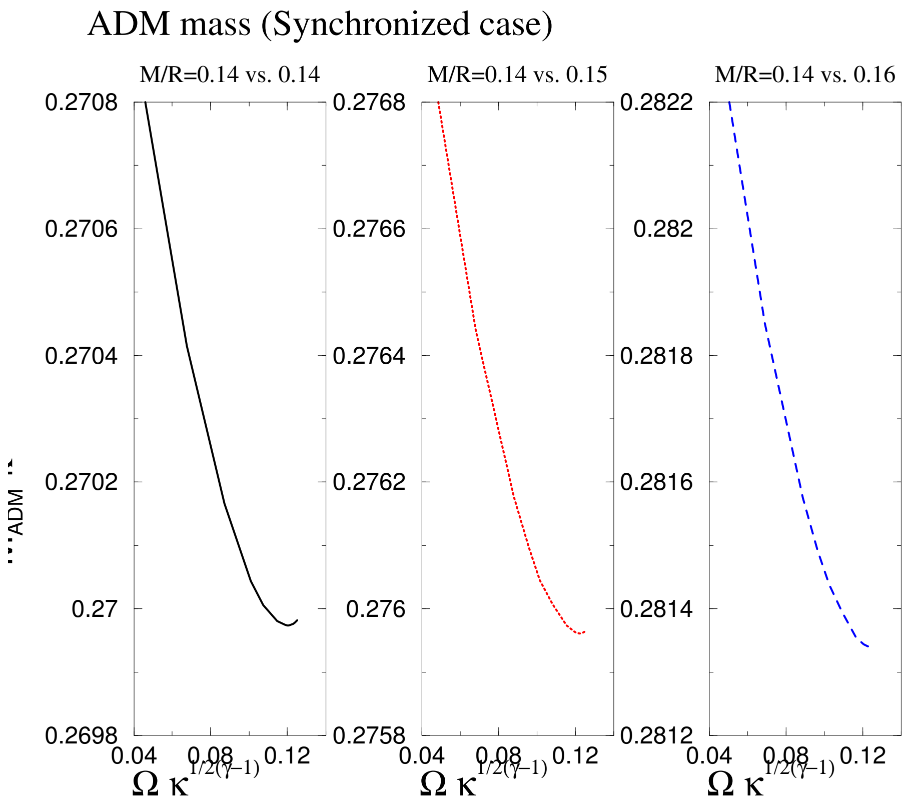

Irrotational case

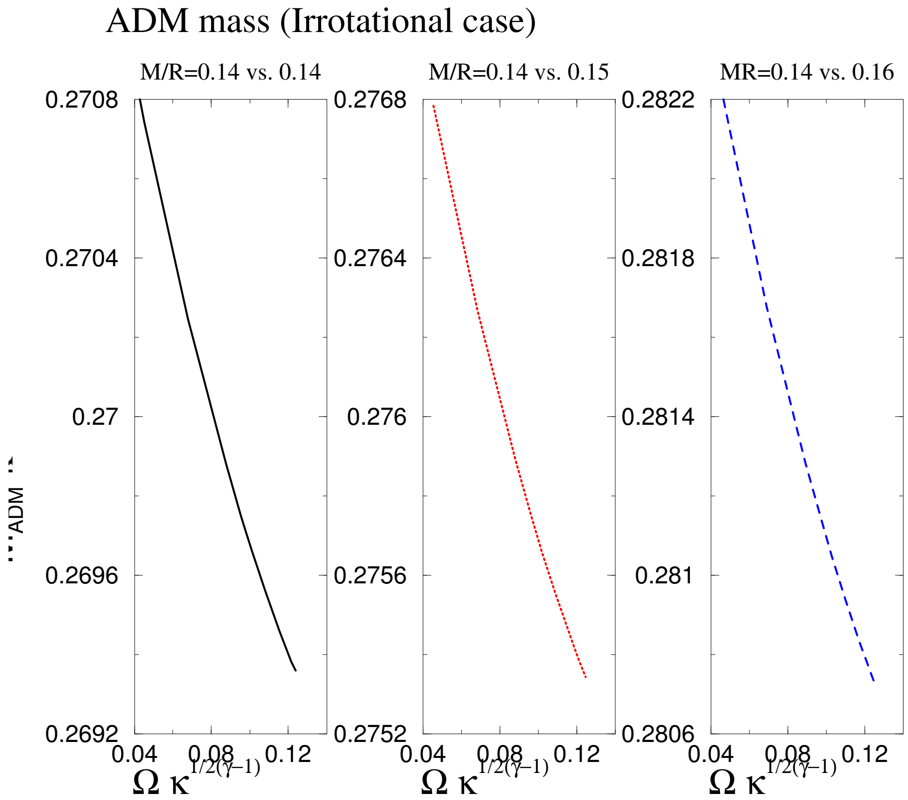

§§6.3 End points of sequences

Identical mass binary systems

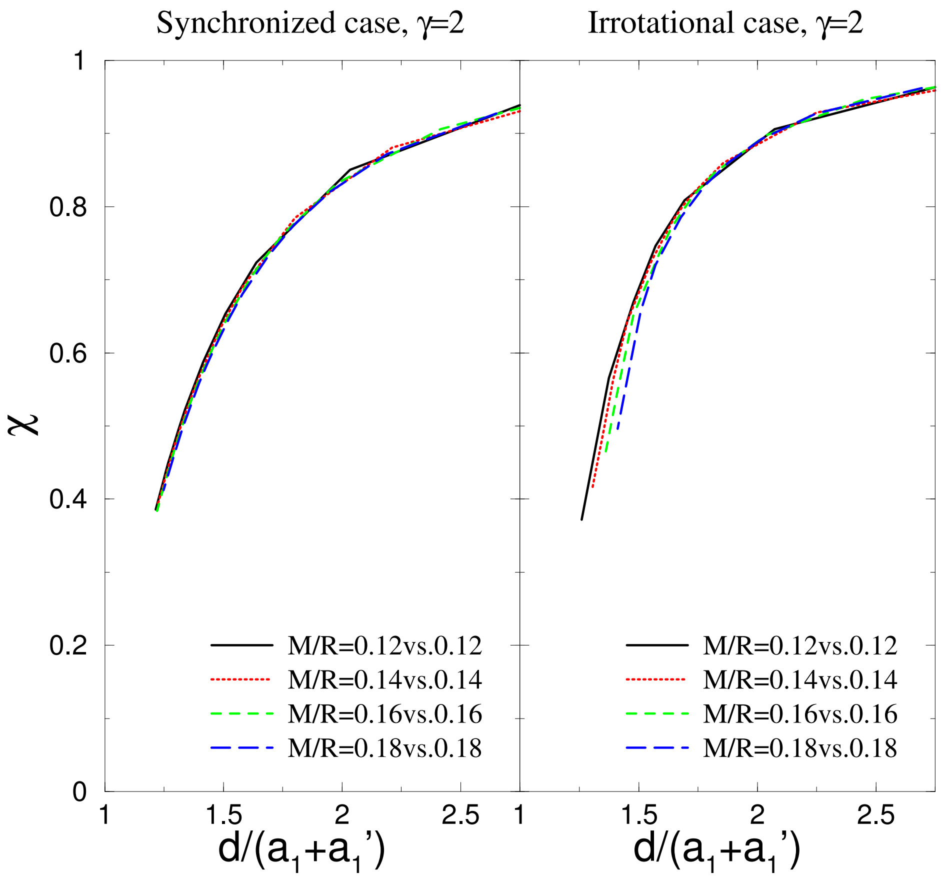

Different mass binary systems

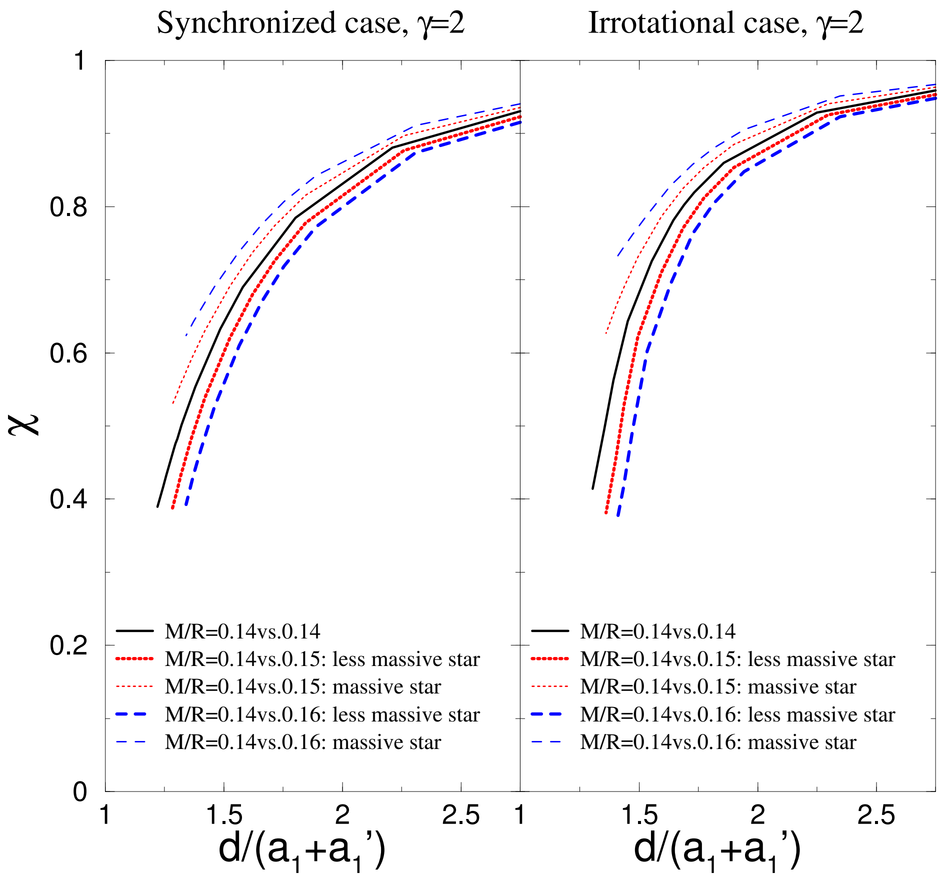

Indicator for mass-shedding limit : $\chi := \dfrac{(\partial H/\partial r)_{\rm eq,comp}}{(\partial H/\partial r)_{\rm pole}}$

Indicator for contact limit : $\dfrac{d}{a_1 + a_1'}$

§§6.4 Central energy density

As a function of the orbital separation

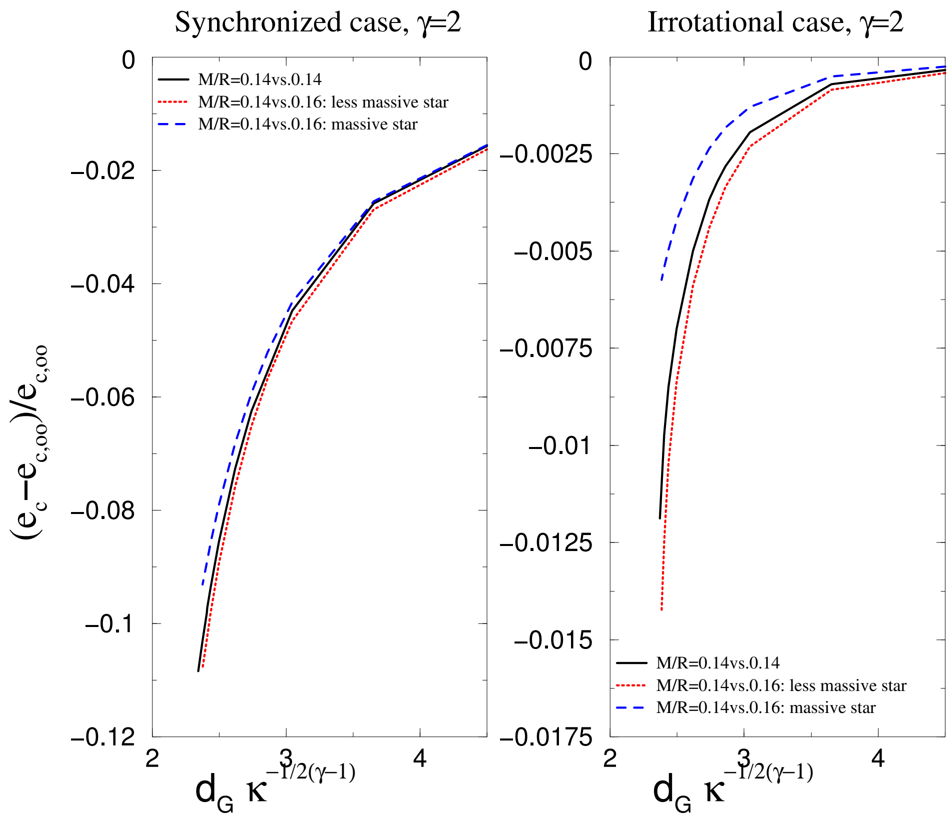

As a function of χ

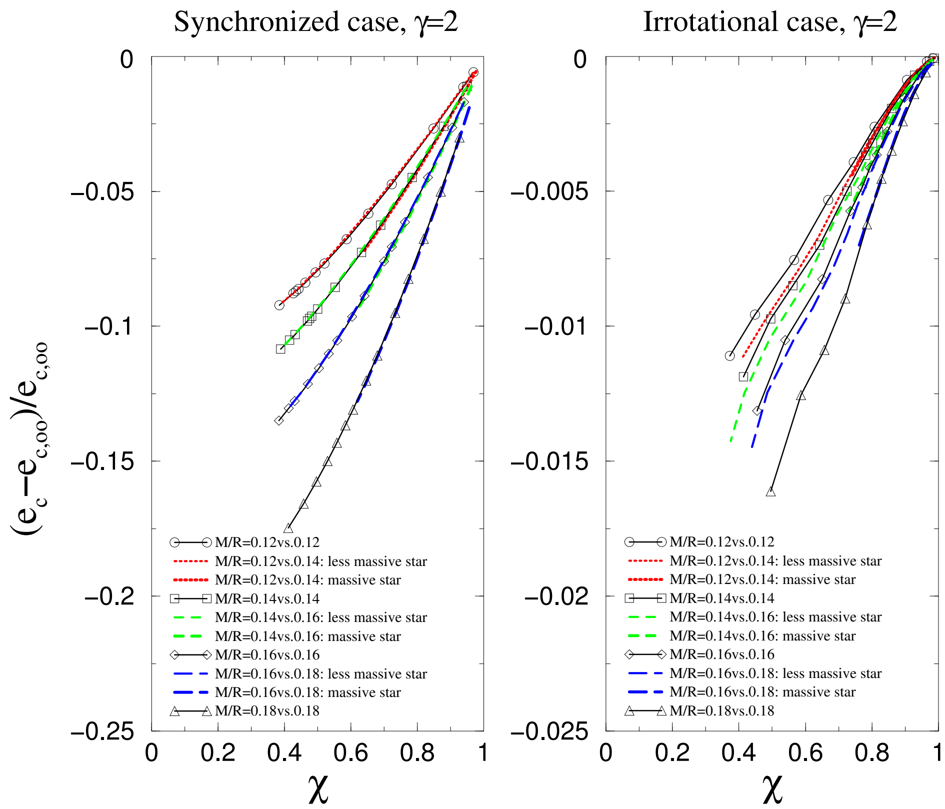

Relative change in central energy density : $\delta e := \dfrac{e_c - e_{c,\infty}}{e_{c,\infty}}$

§§6.5 Axial ratios

Identical mass binary systems

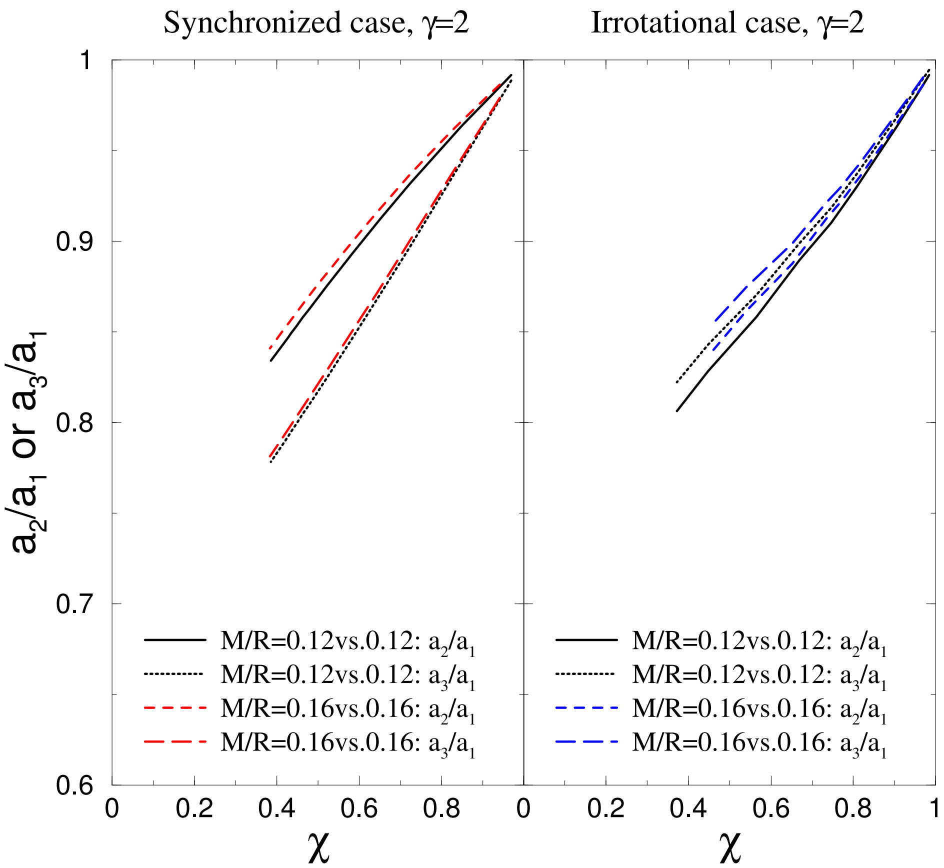

Different mass binary systems

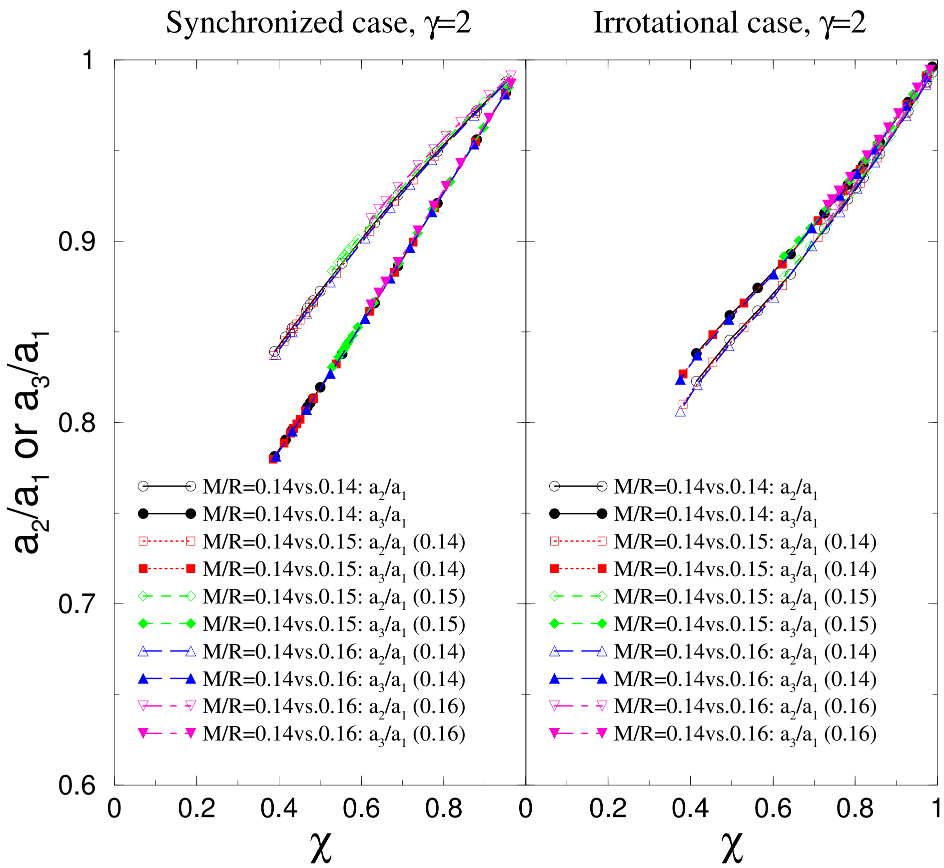

§§6.6 Turning point

Synchronized case

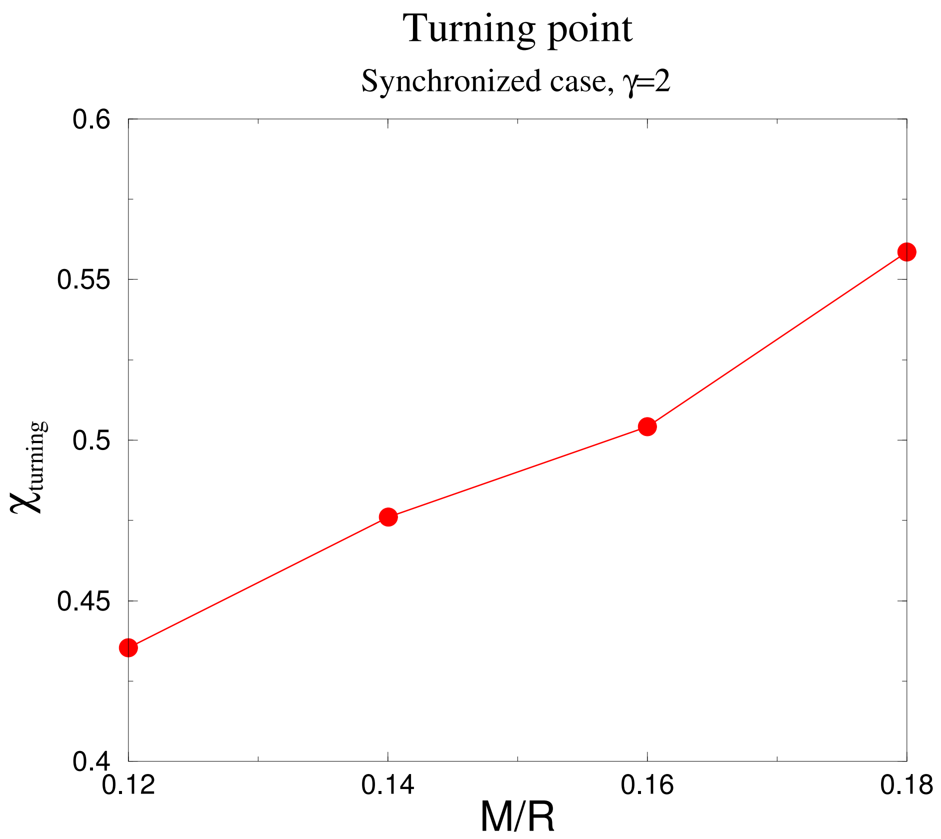

§§6.7 Shift vector

Synchronized case ($\gamma = 2$)

$$\frac{M}{R} = 0.12 \text{ vs. } 0.12$$

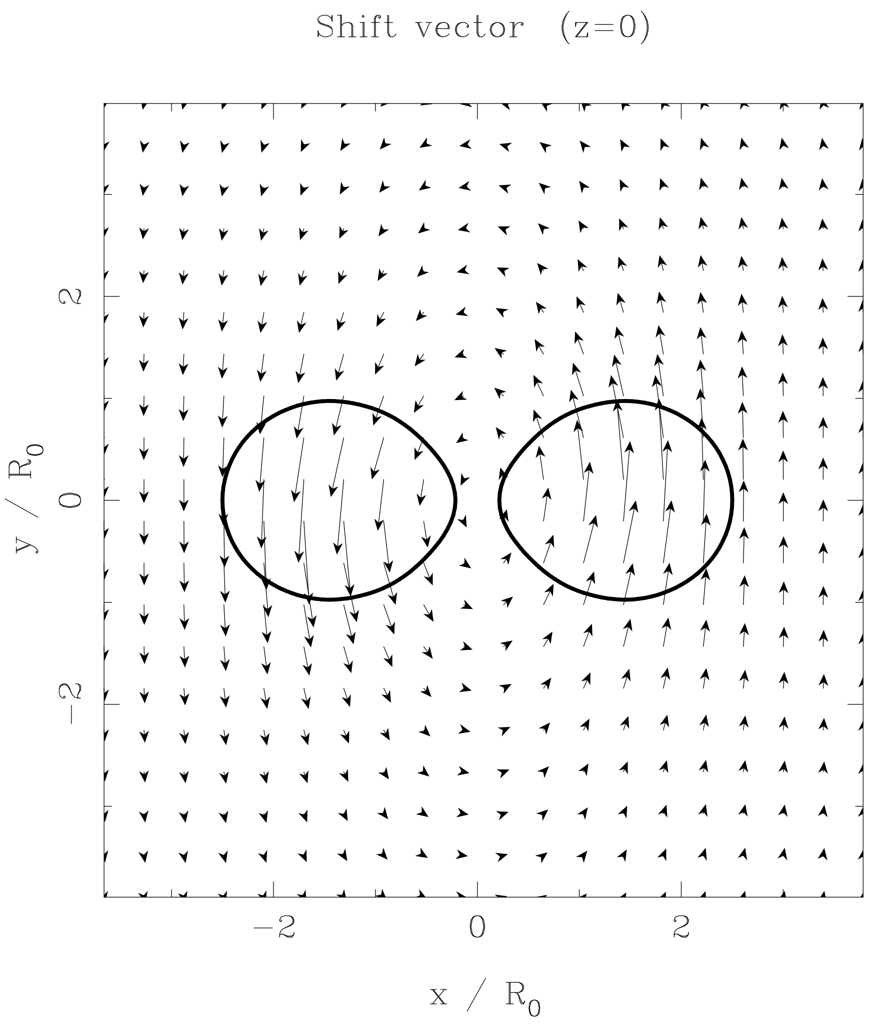

$$\frac{M}{R} = 0.12 \text{ vs. } 0.14$$

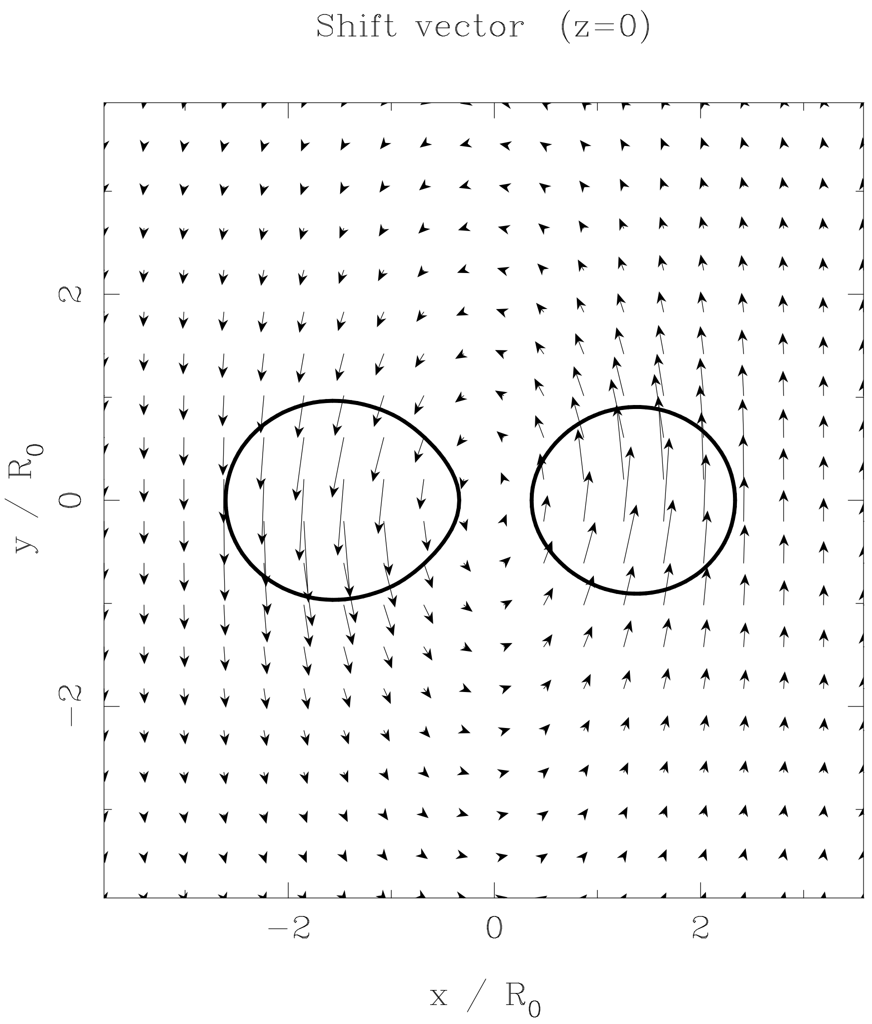

Irrotational case ($\gamma = 2$)

$$\frac{M}{R} = 0.12 \text{ vs. } 0.12$$

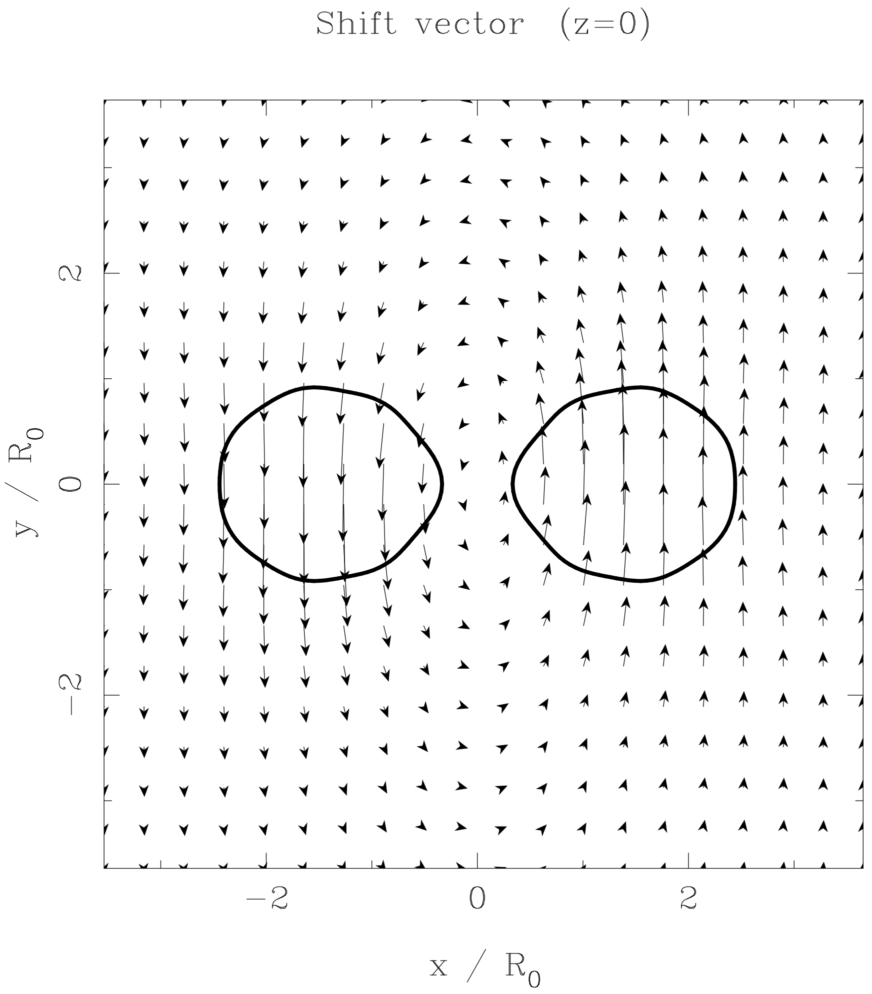

$$\frac{M}{R} = 0.12 \text{ vs. } 0.14$$

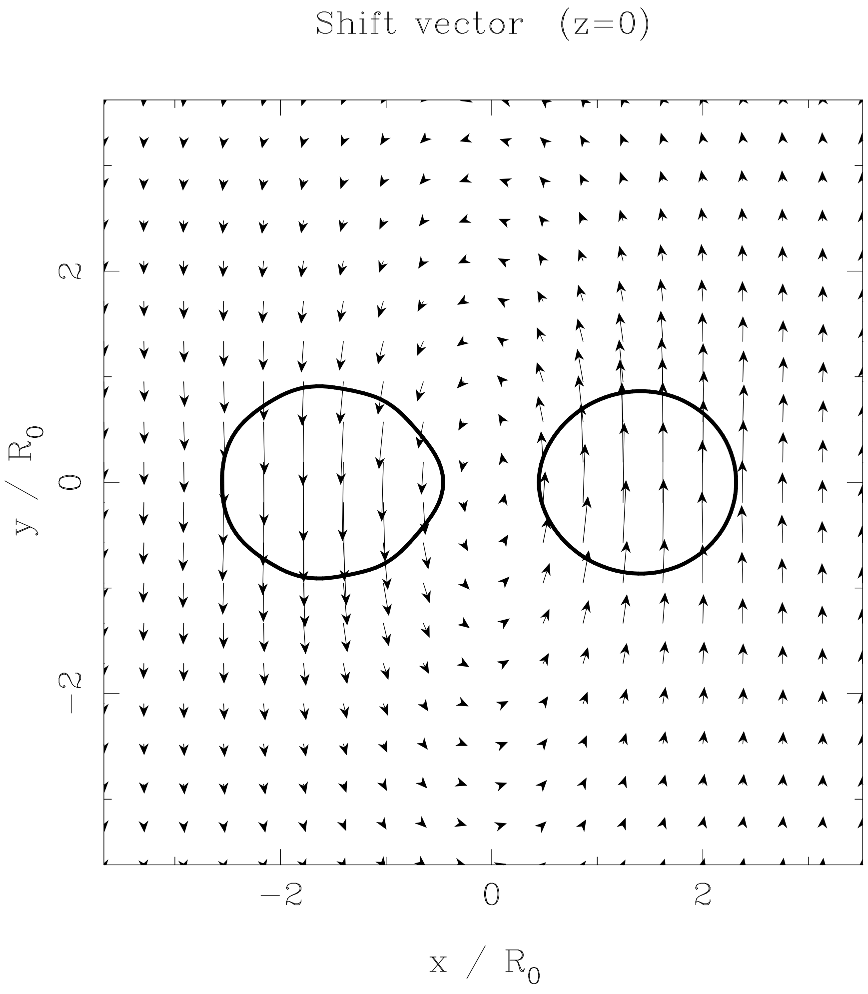

§§6.8 Explanation of the difference in χ

We consider the equal mass binary in Newtonian gravity.

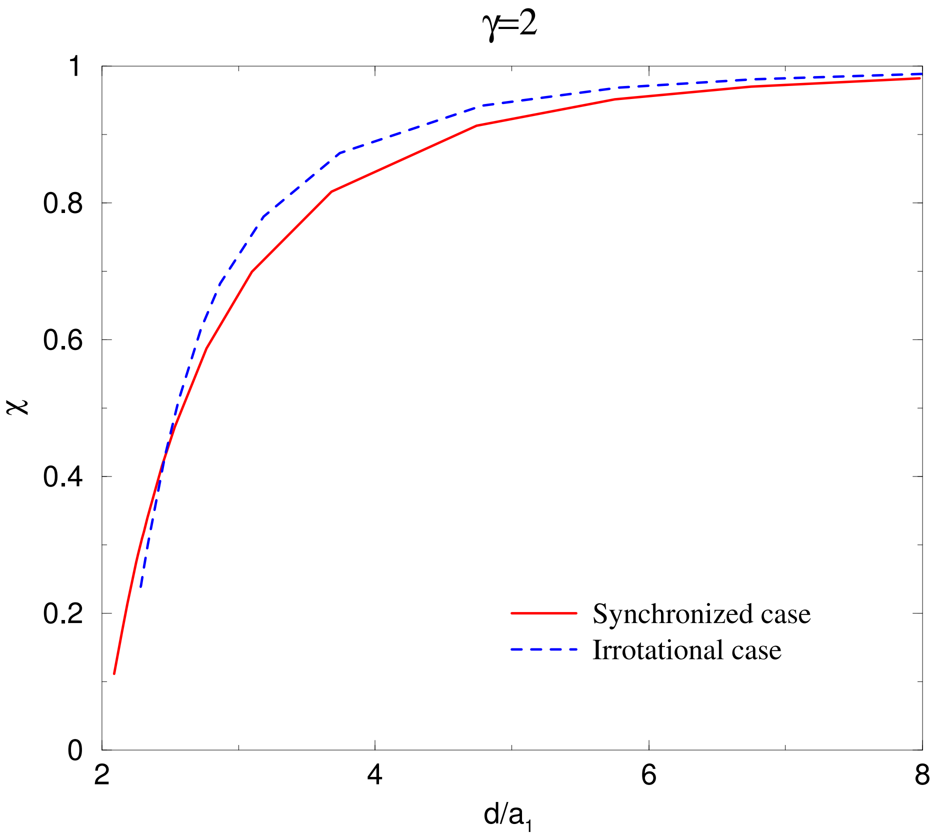

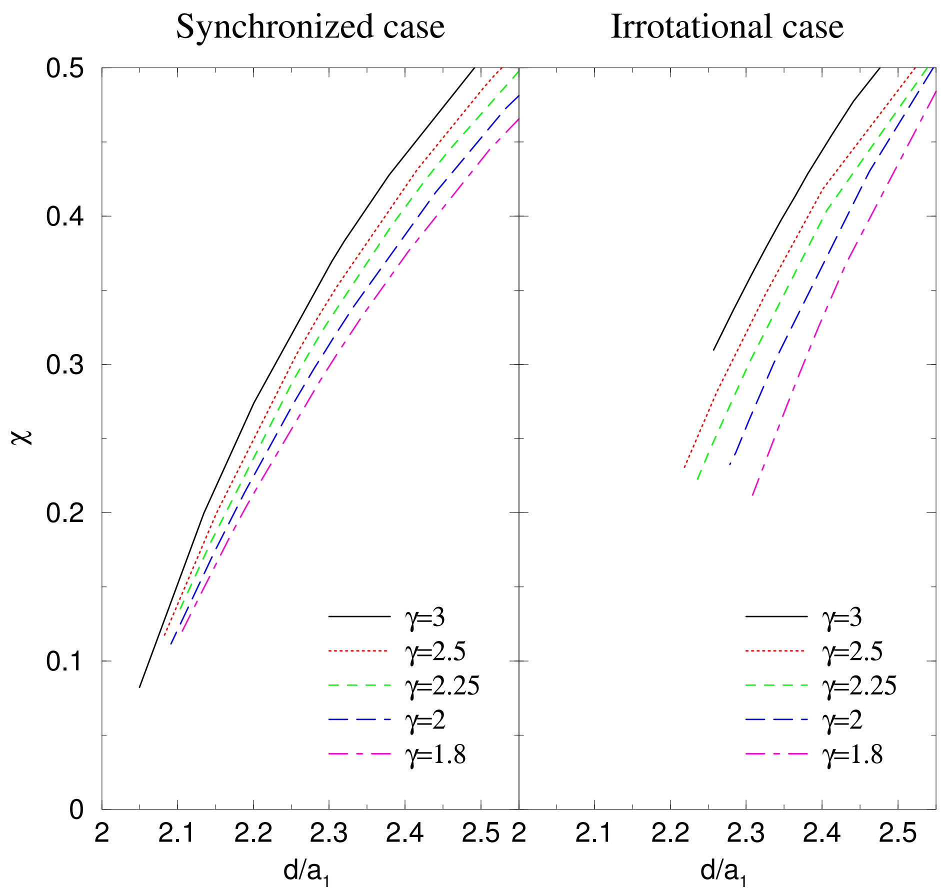

$$\chi := \frac{(\partial H/\partial r)_{\rm eq,comp}}{(\partial H/\partial r)_{\rm pole}}$$

$$\chi^{\rm synch} = \frac{-(\frac{\partial \nu}{\partial x_1})_{\rm eq,comp} + \Omega^2(-\frac{d}{2} + a_1)}{-(\frac{\partial \nu}{\partial z_1})_{\rm pole}}$$

$$\chi^{\rm irrot} = \frac{-(\frac{\partial \nu}{\partial x_1})_{\rm eq,comp} + \Omega^2(-\frac{d}{2} + a_1) - \frac{1}{2}\frac{\partial}{\partial x_1}(\vec{\nabla}\Psi_0 - \mathbf{W}_s)^2|_{\rm eq,comp}}{-(\frac{\partial \nu}{\partial z_1})_{\rm pole}}$$

where $\mathbf{W}_s := \Omega(-y_1,\ x_1,\ 0)$

Difference in χ along a sequence

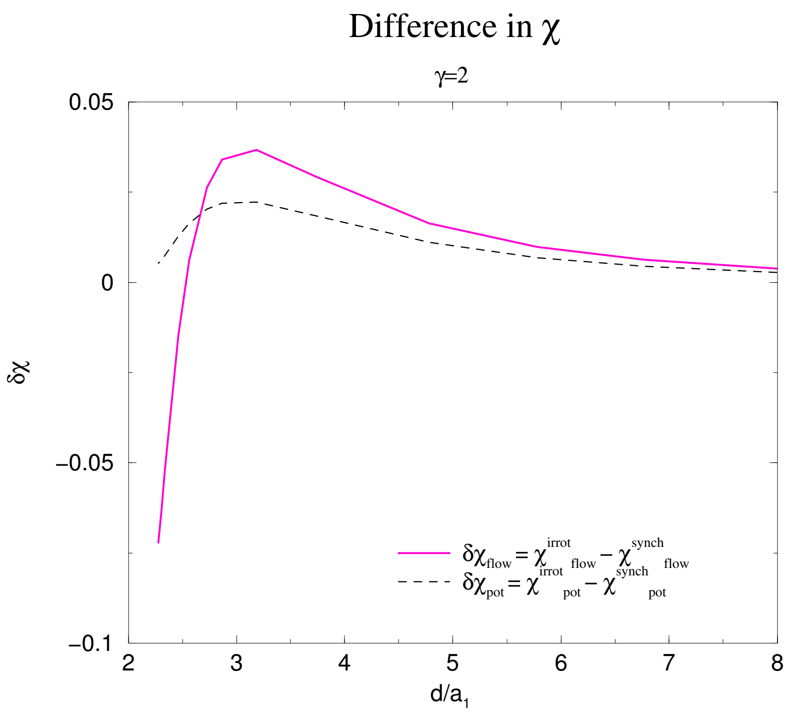

At small separation, the difference in the gravitational force plus centrifugal force is smaller than that in the force related to the internal flow.

Evaluation of the force related to the internal flow

$$F := -\frac{1}{2}\frac{\partial}{\partial x_1}(\vec{\nabla}\Psi_0 - \mathbf{W}_s)^2 = -\Omega^2\left[(f+y_1)\frac{\partial f}{\partial x_1} + (g-x_1)\left(\frac{\partial g}{\partial x_1} - 1\right) + h\frac{\partial h}{\partial x_1}\right]$$

where we assume the form for $\vec{\nabla}\Psi_0$:

$$\vec{\nabla}\Psi_0 = \Omega(f(d,x_1,y_1,z_1),\ g(d,x_1,y_1,z_1),\ h(d,x_1,y_1,z_1))$$

Then the surface value at $(x_1,y_1,z_1) = (a_1,0,0)$ becomes

$$F_{\rm eq,comp} = -\Omega^2 a_1\left[\frac{f(a_1)}{a_1}\frac{\partial f}{\partial x_1}(a_1) + \left(\frac{g(a_1)}{a_1} - 1\right)\left(\frac{\partial g}{\partial x_1}(a_1) - 1\right)\right] \simeq -\Omega^2 a_1\left(\frac{g(a_1)}{a_1} - 1\right)\left(\frac{\partial g}{\partial x_1}(a_1) - 1\right)$$

where we use the fact:

$$f \simeq \Lambda(d)y_1$$

$$g \simeq \Lambda(d)x_1 \qquad \Lambda = O\left[\left(\frac{R_0}{d}\right)^3\right] = \frac{a_1^2 - a_2^2}{a_1^2 + a_2^2}\ :\ \text{ellipsoidal model}$$

$$\Downarrow$$

(i) $\dfrac{g(a_1)}{a_1} < 1$ and $\dfrac{\partial g}{\partial x_1}(a_1) \le 1 \implies$ χ : increase

(ii) $\dfrac{g(a_1)}{a_1} < 1$ and $\dfrac{\partial g}{\partial x_1}(a_1) > 1 \implies$ χ : decrease

$\frac{\partial g}{\partial x_1}$ at $\frac{d}{R_0} = 2.851$

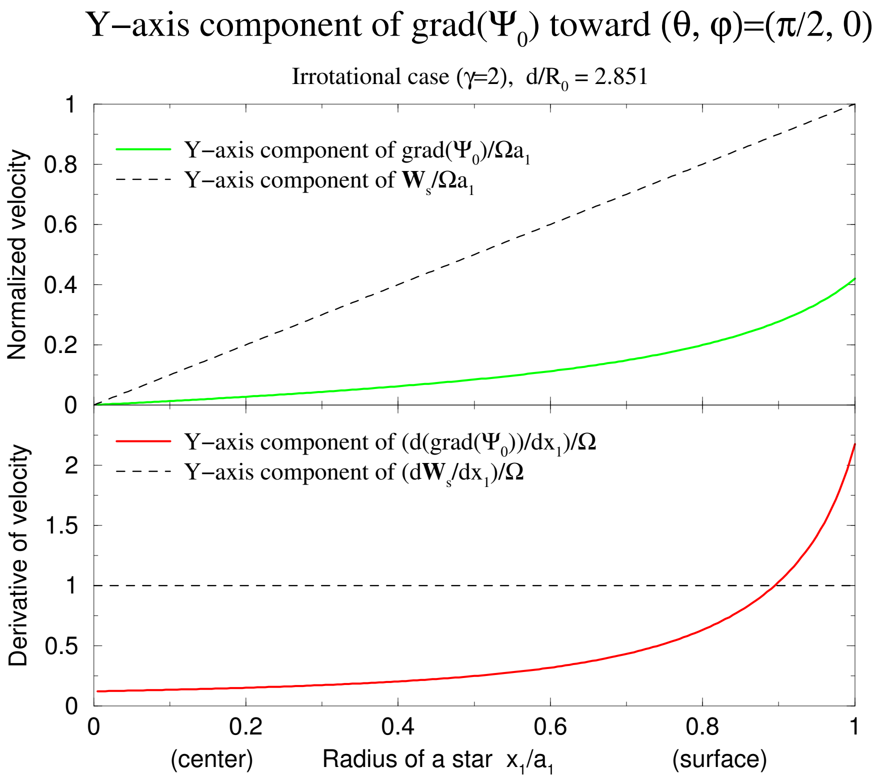

$\frac{\partial g}{\partial x_1}(a_1, 0, 0)$ along a sequence

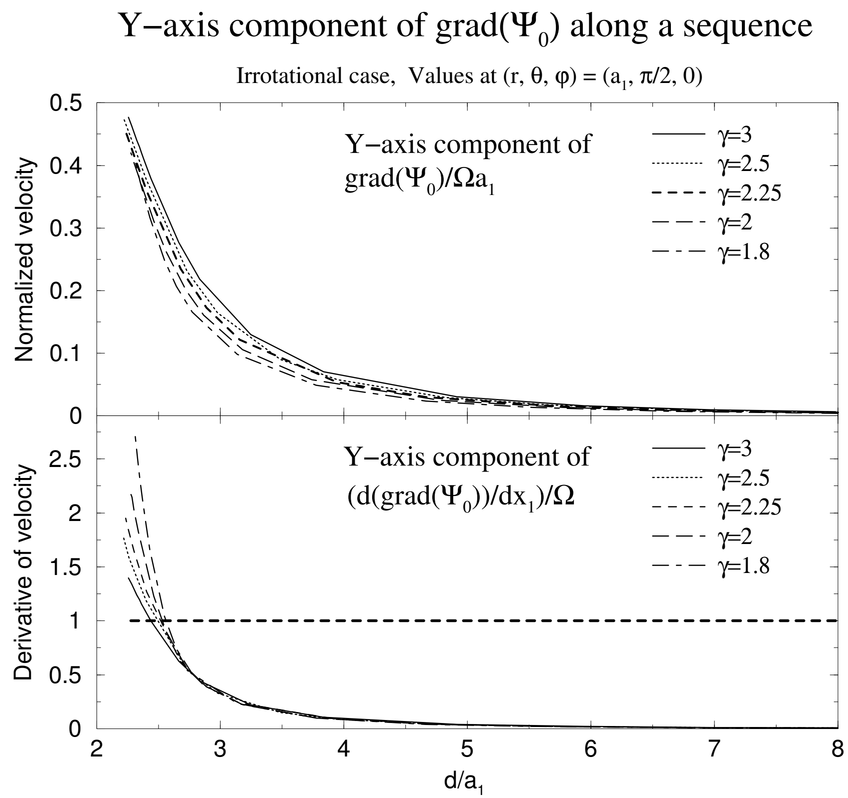

§7. Summary

Constant baryon number sequences of binary neutron stars in quasiequilibrium have been computed in both cases of synchronized and irrotational motion and in both cases of identical and different mass systems.

We have performed a general relativistic treatment, with in the Isenberg-Wilson-Mathews approximation (conformally flat spatial metric).

We have used a polytropic equation of state with an adiabatic index $\gamma = 2$.

(1) Turning point of the ADM mass

- for irrotational binary systems : no turning point
- for synchronized binary systems : one turning point
- is more difficult to be seen for different mass binaries

(2) End point of the sequences

- for synchronized identical star binaries : contact
- for the other types of sequences (synchronized different star binaries, irrotational identical and different star binaries) : mass shedding point

(3) Decrease of the central energy density

- depends on the compactness of the star
- does not depend on that of its companion

(4) Deformation of the star

- is determined by the orbital separation and the mass ratio
- is not affected much by its compactness (in particular for synchronized cases)